

HIGH OUTPUT VOLTAGE THERMOELECTRIC GENERATOR HAVING HIGH-ASPECT-RATIO STRUCTURE

N. Kouma*, T. Nishino, and O. Tsuboi
FUJITSU LABORATORIES LTD., Atsugi, Japan

Abstract: A micro thermocouple with a high output voltage of 0.25 V/K/cm^2 has been achieved with a small diameter of $100 \text{ }\mu\text{m}$ and a high aspect ratio of 3.5. This structure has been accomplished by using a novel fabrication process, which combines the aerosol deposition (ASD) method, a photosensitive glass mold, and post-sintering using hot isostatic pressing (HIP).

Keywords: thermoelectric generator, aerosol deposition, hot isostatic pressing

INTRODUCTION

Micro thermoelectric generators (μTEGs) are one of the promising energy harvesters [1]. They can generate electrical power from thermal energy without needing fuel. It may be possible to achieve completely maintenance-free sensor devices, by using μTEGs to supply electrical power to other integrated devices such as sensors and microchips [2]. It is thought that low output voltages of μTEGs will be one of the most significant problems. The output voltages of the μTEGs are currently lower than the driving voltages of the integrated electronic devices. Therefore, they have to be amplified by using DC-to-DC converters. Although, this conversion losses a lot of energy. For example, the average conversion efficiency is about 20% with the condition that the input voltage is less than 100 mV [3]. That is, more than 80% of the generated output power is wasted as a loss of the amplification. Hence, generating enough voltage is an important requirement for μTEGs for driving sensors with lower output power.

To achieve high output voltages, a μTEG needs both numerous thermocouples and a large temperature difference across the thermocouples. These requirements are achieved by fabricating high-aspect-ratio thermocouples. It is thought to be too difficult to form such structures using semiconductor fabrication processes because both depositing thick films and patterning them are very difficult. Previous works have achieved high-aspect-ratio thermocouples by using MEMS technologies such as wafer bonding, deep reactive ion etching (DRIE), and a thick photoresist [4-6]. We have previously reported a thermocouple having a high aspect ratio of 7, which is enclosed by a photosensitive glass mold, as shown in Fig. 1 [7]. This structure is fabricated by filling through-holes on the mold with thermoelectric powders using the aerosol deposition method (ASD). The high-aspect-ratio thermocouple achieves a high mechanical toughness and

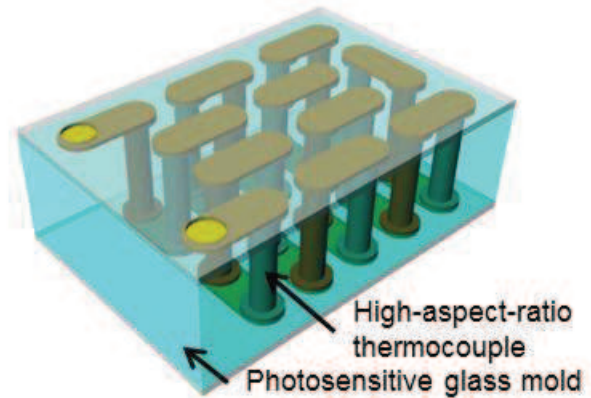


Fig. 1: Schematic diagram of the proposed μTEG .

a high chemical stability because it is protected by the rigid mold. The remaining problem is that the fabricated thermocouple has a higher electrical resistivity than that of a sintered thermocouple. This is because many voids are included in the fabricated thermocouples.

In this paper, we have achieved a micro thermocouple having a high output voltage of 0.25 V/K/cm^2 . The dense thermocouples have been fabricated by applying hot isostatic pressing (HIP).

DESIGN

Figure 2 shows a block diagram of a wireless sensor device including a μTEG . The output voltage of the μTEG is amplified by the DC-to-DC converter before it is supplied to the sensor, microchip, and RF devices. The open circuit voltage and the highest output power generated by the μTEG are expressed in the following equations, where m is the number of thermocouples, α is the Seebeck coefficient, ΔT is the temperature difference across the thermocouples, and R is the internal electric resistance.

$$V = m\alpha\Delta T, P = VI = \frac{V^2}{4R} = \frac{m^2\alpha^2}{4R}\Delta T^2 \quad (1)$$

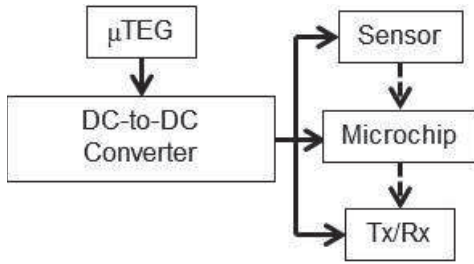


Fig. 2: Block diagram of a wireless sensor device.

This equation shows that many thermolegs as well as a large temperature difference are needed to obtain high output voltage without improving thermoelectric materials. Of course, these are also effective for obtaining high output power. To put it briefly, these requirements are overcome by fabricating small and high-aspect-ratio thermolegs because the former achieves highly integrated thermolegs and the latter realizes a high thermal resistance. Accurately, thermolegs have optimum shapes according to their operating conditions. Glatz et al has estimated details about optimum shapes of thermolegs enclosed by insulators [6].

In this paper, high-aspect-ratio thermolegs are achieved with a high mechanical toughness by enclosing them in a rigid glass mold. Figure 3 shows a calculated result to demonstrate the toughness of the enclosed thermoleg using a FEM simulation. The Von Mises stress of the enclosed thermoleg is compared to the unenclosed thermoleg with various aspect ratios. The length of the thermolegs is varied from 25 μm to 500 μm with their width fixed at 50 μm , corresponding to aspect ratios from 0.5 to 10. The area ratio of the thermoleg and the mold is 1:9. The load conditions are as follows. A constant load of 100 MPa is applied to the side surface of the top substrate to bend the thermoleg. The bottom substrate is fixed. First, the maximum stress of the unenclosed thermoleg is more than 130 MPa, and increases

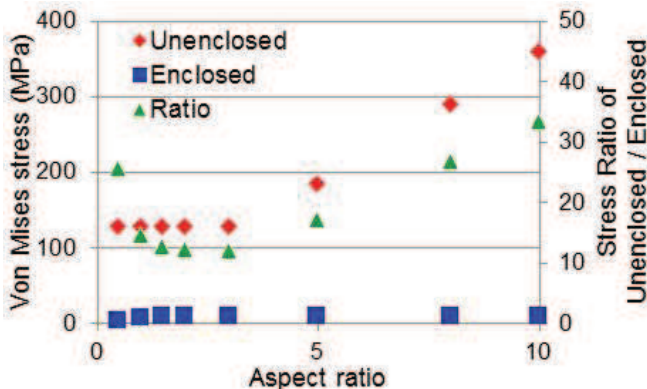


Fig. 3: Calculated stress concentration of various structures with various aspect ratios.

rapidly at an aspect ratio of more than 3. The stress concentration point also changes from the top area to the bottom area at the same aspect ratio. It is thought that the bending moment increases rapidly at an aspect ratio of more than 3. Then, the maximum stress concentration of the enclosed thermoleg is reduced to only 8.7 MPa at the aspect ratio of 3. Furthermore, this value almost keeps even if the aspect ratio increases. The important point to note is that the advantage of the enclosed thermolegs becomes greater as the aspect ratio increases. For example, the enclosed structure has more than 30 times the toughness than the unenclosed structure at an aspect ratio of 10.

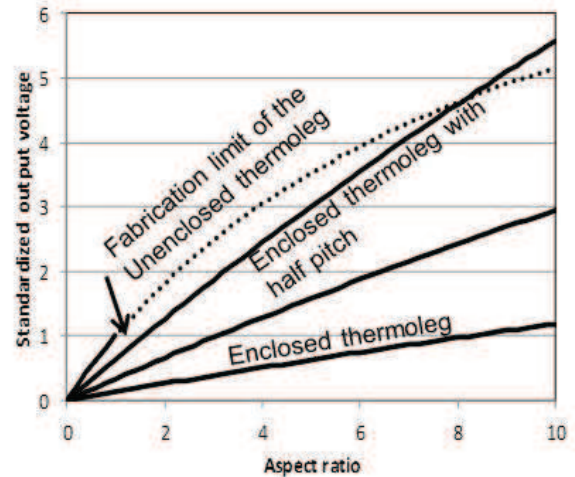


Fig. 4: Calculated open circuit voltages of the enclosed structure compared with the unenclosed structure.

On the other hand, a problem that should be considered is thermal loss via the mold. Figure 4 shows the estimated output voltages of the enclosed thermoleg, compared with that of the unenclosed thermoleg. They are calculated on the same conditions of thermoleg shapes and the heat transfer coefficient of the heat sink. The output voltages are standardized by an unenclosed thermoleg having an aspect ratio of 1. This graph shows that the output voltage decreases by adding the mold. This is because the temperature difference decreases due to the thermal loss via the mold. The enclosed structure needs 8 times the aspect ratio to obtain the same output voltage of the unenclosed structure. It is estimated that 5.5 times the output voltage can be obtained by fabricating the enclosed structure with both an aspect ratio of 10 and half pitch. This shape can be achieved by improving the fabrication process.

FABRICATION

The details of the process to fabricate μTEGs are shown in Fig. 5. The 350- μm -thick photosensitive

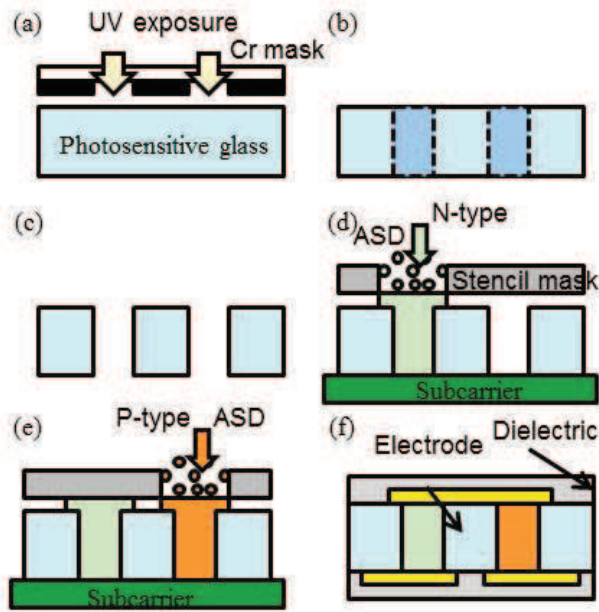


Fig. 5: Fabrication process of a μ TEG.

glass substrate (PEG-3R, Hoya) is used as a mold substrate. First, the substrate is exposed to UV light at 20 mW/cm^2 for 150 s via a Cr mask (Fig. 3(a)). This is followed by two-step N_2 annealing in a high-temperature furnace at $500 \text{ }^\circ\text{C}$ for 1 h and at $590 \text{ }^\circ\text{C}$ for 2 h (Fig. 3(b)). The substrate is dipped in a diluted HF solution (DI water: HF (49%) = 4:1) until the through-holes are completely formed in the exposed area (Fig. 3(c)). The exposed area has 20 times more etching ratio than the unexposed area. The photosensitive glass mold is fabricated after dicing the wafer into chips. Then, the mold chip is precisely aligned and temporarily bonded with the stencil mask that is fabricated by photolithography, etched with deep reactive ion etching (DRIE), and the photoresist is removed using a 100- μm -thick silicon substrate. The stacked chip is mounted on a carrier substrate such as a silicon substrate, and introduced into the ASD chamber to be filled with Bi_2Te_3 powder as an n-type semiconductor material (Fig. 3(d)). In the ASD chamber, Bi_2Te_3 powders are accelerated with compressed air and injected from the nozzle into the substrate. Dense thermolegs are formed in the through-holes on the mold by the kinetic energy of the powders. At this time, the through-holes for p-type thermolegs are selectively masked by the stencil mask. After changing the stencil mask, $\text{Bi}_{0.3}\text{Sb}_{1.7}\text{Te}_3$ powders are similarly filled in the through-holes for p-type thermolegs (Fig. 3(e)). After that, a post-processing is applied to enhance the thermoelectric property of the fabricated thermolegs. After polishing both the surfaces of the mold, electrodes of Cu/Cr are formed on both the surfaces using stencil masks (Fig. 3(f)).

Finally, dielectric material layers are deposited on both surfaces (Fig. 3(g)). By using the described processes, the μTEG is completed.

DISCUSSION

A high electrical resistivity is the main problem of the ASD thermoleg. Therefore, it is compared after various post-processing, as shown in Fig. 6. First, the ASD films deposited on a flat surface are investigated. As-deposited films have low electrical resistivities of $11 \text{ m}\Omega\text{cm}$ and $4.4 \text{ m}\Omega\text{cm}$ for Bi_2Te_3 and $\text{Bi}_{0.3}\text{Sb}_{1.7}\text{Te}_3$, respectively, which are only about ten times higher than that of the sintered thermolegs fabricated using these materials. Furthermore, these values are suppressed to $0.5 \text{ m}\Omega\text{cm}$ and $2.0 \text{ m}\Omega\text{cm}$ after post-annealing with $400 \text{ }^\circ\text{C}$ in a N_2 atmosphere. The Seebeck coefficients of these films are $150 \text{ } \mu\text{V/K}$ and $190 \text{ } \mu\text{V/K}$, respectively, which are as same as those of the starting materials. It is demonstrated that the ASD film achieves as good thermoelectric properties as the sintered thermoleg by the assistance of the post-annealing.

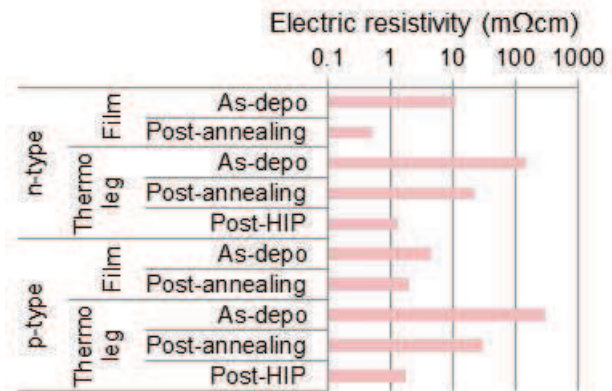


Fig. 6: Improvements of electrical resistivities compared ASD films and ASD thermolegs.

Then, the thermoelectric properties of the high-aspect-ratio thermolegs are compared with those of the ASD films. The fabricated thermoleg has a $100\text{-}\mu\text{m}$ diameter and $350\text{-}\mu\text{m}$ height. The electric resistivity of as-filled Bi_2Te_3 thermoleg is about $147 \text{ m}\Omega\text{cm}$, which is about 10 times higher than that of the as-deposited film. This is improved only to $22 \text{ m}\Omega\text{cm}$ after the post-annealing. Similarly, the electrical resistivity of $\text{Bi}_{0.3}\text{Sb}_{1.7}\text{Te}_3$ is $30 \text{ m}\Omega\text{cm}$. It is said that the ASD thermolegs cannot achieve good electrical properties only by the post-annealing. Therefore, hot isostatic pressing (HIP) is achieved to pressurize the thermolegs. Here, a pressure of 196 MPa is added with the Ar annealing at $400 \text{ }^\circ\text{C}$. By applying HIP, the

thermolegs achieve low electric resistances of 1.3 mΩcm and 1.7 mΩcm for Bi₂Te₃ and Bi_{0.3}Sb_{1.7}Te₃, respectively. It is demonstrated that the electric resistivity of the ASD thermolegs is improved to the same value of that of the ASD films. Figure 7 compares cross-sectional SEM images of the thermolegs after the annealing (a) and HIP (b). There are many voids in the annealed thermoleg, as shown in Fig. 7(a). The interfacial resistances at grain boundaries seem to result in the high resistance. This is because the accelerated powders loss their kinetic energy in deep through-holes. On the other hand, it is obvious that the voids can be decreased effectively by HIP, as shown in Fig. 7(b).

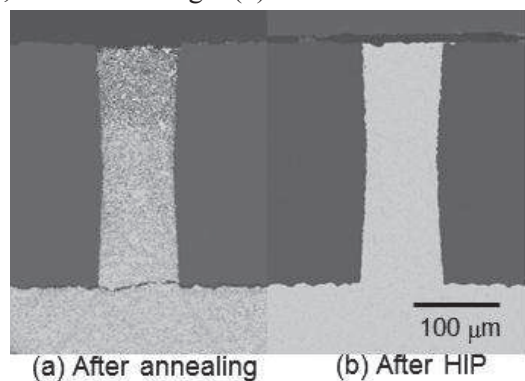


Fig. 7: Cross-sectional SEM images of fabricated thermolegs after annealing (a) and HIP (b).

Figure 8 shows the output properties of one fabricated thermocouple. They are fabricated by the process as shown in Fig. 5 and applied the HIP with the condition of 400 °C and 196 MPa. The thermoleg shape is 100 μm in diameter, 350 μm in height, and 240 μm in pitch. First, measured internal resistance of the thermocouple is about 1.0 Ω, which corresponds with the electrical resistivity of 1.2 mΩcm. The Seebeck coefficient of the thermocouple is 290 μV/K. This is a little lower than 340 μV/K, which is the total value of the ASD films evaluated above. This reason is thought that the ASD process cannot achieve a completely separation of n- and p-type powers. The maximum output power and the output open circuit voltage are 5.73 nW/K² and 0.30 mV/K, respectively. These results imply that 480 μW/cm² and 2.5 V/cm² will be achieved with a temperature difference of 10 K by connecting a large number of thermolegs. This will be able to drive microcontrollers without the assistance of converters.

RESULTS

We have developed micro thermocouples having a high output voltage of 0.25 V/K/cm² with a small

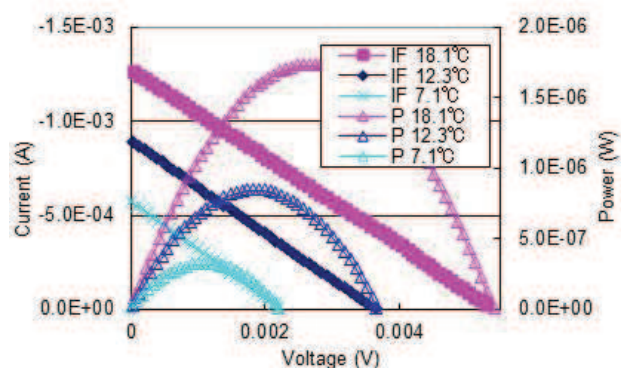


Fig. 8: Thermoelectric properties of a fabricated thermoleg.

diameter of 100 μm and a high aspect ratio of 3.5. It is demonstrated that the high-aspect-ratio thermoleg achieves the same thermoelectric properties as the sintered thermolegs by using ASD followed by HIP. We expect that a high output voltage of more than 1 V will be achieved by using this μTEG.

REFERENCES

- [1] M. Kishi, H. Nemoto, T. Hamao, M. Yamamoto, S. Sudou, M. Mandai and S. Yamamoto 1999 Micro-Thermoelectric Modules and Their Application to Wristwatches as an Energy Source *Proc. 18th ICT* pp. 301-307.
- [2] H. Böttner, J. Nurnus, A. Schubert, and F. Volkert 2007 New high density micro structured thermogenerators for stand alone sensor systems, *Proc. 26th ICT* pp. 306-309.
- [3] <http://www.alldatasheet.com/datasheet-pdf/pdf/314520/LINER/LTC3108EDE.html>
- [4] H. Böttner, J. Nurnus, A. Gavrikov, G. Kuhner, M. Jagle, G. Kunzel, D. Eberhard, G. Plescher, A. Schubert, and K-H. Schlereth 2004 New thermoelectric components using microsystem technologies *J. Micromech. Syst.*, vol.13 (2004), pp. 414-420.
- [5] J-F. Li, S. Tanaka, T. Umeki, S. Sugimoto, M. Esashi, and R. Watanabe 2003 Microfabrication of thermoelectric materials by silicon molding process *Sensors and Actuators A: Physical*, 108 (2003), pp. 97-102.
- [6] W. Glatz, S. Muntwyler, and C. Hierold 2006 Optimization and fabrication of thick flexible polymer based micro thermoelectric generator *Sensors and Actuators A: Physical*, 132 (2006), pp. 337-345.
- [7] N. Kouma and O. Tsuboi 2011 Highly integrated and stiffened micro thermocouples fabrication using glass molds selectively filled with nanopowders *Technical Digest PowerMEMS 2011* pp. 82-85